STRUCTURAL TOPOLOGY OPTIMIZATION BASED ON HYBRID OF PIECEWISE CONSTANT LEVEL SET METHOD AND ISOGEOMETRIC ANALYSIS

M. Khatibinia[*, †] and M. Roodsarabi
Department of Civil Engineering, University of Birjand, Birjand, Iran

ABSTRACT

The present study proposes a hybrid of the piecewise constant level set (PCLS) method and isogeometric analysis (IGA) approach for structural topology optimization. In the proposed hybrid method, the discontinuities of PCLS functions is used in order to present the geometrical boundary of structure. Additive Operator Splitting (AOS) scheme is also considered for solving the Lagrange equations in the optimization problem subjected to some constraints. For reducing the computational cost of the PCLS method, the Merriman–Bence–Osher (MBO) type of projection scheme is applied. In the optimization process, the geometry of structures is described using the Non–Uniform Rational B–Splines (NURBS)–based IGA instead of the conventional finite element method (FEM). The numerical examples illustrate the efficiency of the PCLS method with IGA in the efficiency, convergence and accuracy compared with the other level set methods (LSMs) in the framework of 2–D structural topology optimization. The results of the topology optimization reveal that the proposed method can obtain the same topology in lower number of convergence iteration.

1. INTRODUCTION

Topology optimization has been proposed in order to determine an optimal layout of a structure or the best distribution of material in the conceptual design stage [1]. For the topology optimization, several methods have been developed in the past decades, such as Optimality Criteria (OC) methods [2, 3], the approximation methods [4–6], the Method of

---

[*]Corresponding author: Department of Civil Engineering, University of Birjand, Birjand, Iran
[†]E-mail address: m.khatibinia@birjand.ac.ir (M. Khatibinia)

Moving Asymptotes (MMA) [7–9], Evolutionary Structural Optimization (ESO) method [10] and even more heuristic methods such as genetic algorithm [11] and Ant colony [12]. In recent years, the level set method (LSM) has been proposed for the topology optimization of structures, which utilizes a flexible implicit description of the material domain [13]. The main idea of the LSM approach is to apply an implicit boundary describing model to parameterize the geometric model, and the boundary of a structure is embedded in a high–dimensional level set function [14]. The LSM not only fundamentally avoid meshing dependence, but also maintain smooth boundaries and distinct material interfaces during the topological design process [15]. The capability of the standard LSM has been demonstrated in solving many different types of structural shape optimization problems with drastic topological changes [15]. However, the existence of some drawbacks has remained in the standard LSM such as: (1) The final optimal design highly depends on the initial guess of holes inside the design domain. (2) The time step must be considered to be a small enough value to satisfy the Courant–Friedrichs–Lewy (CFL) condition, and it leads to a time–consuming optimization process with many iterations [16]. Therefore, several alternative LSMs have been proposed to eliminate the drawbacks of the standard LSM [16–20].

A piecewise constant level set (PCLS) approach as a variant of the standard LSM was proposed for the image segmentation, shape recovery or elliptic inverse problems [21]. In the PCLS approach, distinct constant values are selected for each sub–domain of the computational domain. In the PCLS method, an arbitrary number of sub–domains can be identified using only one discontinuous piecewise constant level set function. Furthermore, the interfaces between sub–domains are represented implicitly by the discontinuity of a set of characteristic functions of the sub–domains [21]. The PCLS method in comparison with the standard LSM does not required solving the Hamilton–Jacobi partial differential equation and the use of the signed distance function as the initial one. In recent years, the PCLS method has been utilized for the topology optimization [22, 23] and the shape and topology optimization and the Laplace equation in 2–D domain [19].

Most of topology optimization methods have utilized the conventional finite element method (FEM) for structural analysis and sensitivity calculation. In general, the method suffers two serious drawbacks due to a fixed FE grid used for material representation and numerical analysis. The first one is that design results are highly dependent on the initial fixed FE grid [24]. In the level set–based approaches, a fixed FE rid is applied to define level set values at nodes and to analyze design models. The second drawback is that the topology optimization based on FEM requires the high post–processing effort in converting the optimized result to the computer–aided design (CAD) model. Using an alternative analysis method without fixed grid can overcome the first drawback. Also, unifying analysis and design models defined with CAD data have been proposed to eliminate the second drawback. In these regards, the isogeometric analysis (IGA) approach has been developed as a promising alternative to FEM in topology optimization [25–27]. IGA based on Non–Uniform Rational B–Splines (NURBS) basis function can be applied for both the solution field approximation and the geometry description. This leads to the ability of modeling complex geometries accurately.

In this study, a hybrid of the PCLS method and IGA is proposed for the 2–D structural topology optimization. For defining the geometrical boundary of structure, the discontinuities of PCLS functions is used in the proposed hybrid method. The Lagrange

equations in the PCLS method is also solved by Additive Operator Splitting (AOS) scheme. In order to reduce the computational cost of the PCLS method, the Merriman–Bence–Osher (MBO) type of projection scheme is applied in the PCLS method. Furthermore, in the topology optimization procedure the NURBS based–IGA approach is considered instead of the conventional FEM. In fact, in the IGA approach control points play the same role with nodes in FEM and B–Spline basis functions are adopted as shape functions of FEM for the analysis of structure. Boundary conditions are directly imposed on control points. Numerical integration is implemented almost same with FEM in order to transform the parametric domain to master element for Gauss quadrature. In the topology optimization procedure, the design model is computed using a fixed isogeometric mesh which is unchanged during the topology optimization procedure. Hence, in this study the popular "Ersatz material" approach [15] is adopted in order to avoid the time–consuming re–meshing process of design model topology optimization procedure. In this study, three numerical examples are represented to demonstrate the capability and performance of the proposed method. The optimal results of the proposed method are also compared with the other LSMs to indicate the efficiency and accuracy of the proposed method. Finally, the results of the structural topology optimization demonstrate that the same optimum topology can be obtained by the proposed method in less iterations. Therefore, the proposed method can be considered as the efficient method in the 2–D structural topology optimization.

2. TOPOLOGY OPTIMIZATION WITH THE PCLS METHOD

2.1 Piecewise constant level set method

The piecewise constant level set (PCLS) method was developed by Lie *et al.* [28]. Based on the PCLS method, the domain Ω is partitioned into *n* sub–domains $\{\Omega\}_{i=1}^{n}$ such as [28]:

$$\Omega = \bigcup_{i=1}^{n} \Omega_i \cup \Gamma \tag{1}$$

where Γ is the union of the boundaries of the sub–domains.

In order to identify each of the sub–domains, a piece–wise constant function $\phi : \Omega \to R$ is defined on the open and bounded domain. A distinct constant value within each sub–domain is selected as [28]:

$$\phi(x) = i \quad ; \quad x \in \Omega_i \quad (i = 1, 2, ..., n) \tag{2}$$

In this method, just one function is required for identifying all the sub–domains in Ω. Each sub–domain Ω_i can be associated with a characteristic function $\psi(x_i)$, such that $\psi_i = 1$ in Ω_i and $\psi_i = 0$ elsewhere as long as Eq. (2) holds. The characteristic functions can be constructed in the following form [28]:

$$\psi_i = \frac{1}{\alpha_i} \prod_{j=1, j \neq i}^{n} (\phi - j) \quad \text{and} \quad \alpha_i = \prod_{k=1, k \neq i}^{n} (i - k) \tag{3}$$

For representing the different properties in each sub–domain $\rho = c_i$ in Ω_i, a piecewise density function is defined as follow [28]:

$$\rho(\phi) = \sum_{i=1}^{n} c_i \psi_i (\phi) \tag{4}$$

and

$$K(\phi) = (\phi - 1)(\phi - 2)...(\phi - n) = \prod_{i=1}^{n} (\phi - i) \tag{5}$$

In order to guarantee that there is no vacuum and overlap between the different phases, It is necessary to consider a piecewise constant constraint i.e. $K(\phi) = 0.$ With the simple structure of the characteristic functions, the volume and the perimeter of each subdomain Ω_i are also measured by [28]:

$$|\Omega_i| = \int_{\Omega} \psi_i dx \quad \text{and} \quad |\partial\Omega_i| = \int_{\Omega} |\nabla \psi_i| dx \tag{6}$$

One of the main advantages of the PCLS method is to only use one level set function for representing multi–phases. In this study, the PCLS method is implemented in two phases for the topology optimization problems. Hence, the piecewise constant density function is defined in two phases as:

$$\rho(\phi) = -c_1 (\phi - 2) + c_2 (\phi - 1) \tag{7}$$

where c_1 and c_2 are the specified characteristic values of the void material, with $c_1 = 0,$ and the solid material with $c_2 = 1.$ In order to ensure the convergence of the level set function ϕ to a unique value in each sub–domain, the piecewise constant constraint is defined as:

$$K(\phi) = 0 \quad \text{and} \quad K(\phi) = (\phi - 1)(\phi - 2) \tag{8}$$

This indicates that every point in the design domain must belong to one phase, and there is no vacuum and overlap between different phases.

2.2 Topology optimization based on the PCLS model

The topology optimization process can operate on the PCLS model ϕ presented in the previous section. In this study, the topology optimization problem is presented by

minimizing the mean compliance of a structure of two–phase material (i.e. solid and void). Hence, the topology optimization problem of a structure can be defined as follows [16]:

$$
\text{Minimize:} \quad J(u,\phi) = \int_\Omega \rho(\phi) F(u) d\Omega + \beta \int_\Omega |\nabla \phi| d\Omega
$$

$$
\text{subjected to:} \quad H_1 = \int_\Omega \rho(\phi) dx - V_0 \leq 0
$$

$$
H_2 = K(\phi) = 0
$$

$$
a(u,v,\phi) = l(v,\phi) \tag{9}
$$

$$
a(u,v,\phi) = \int_\Omega \rho(\phi) E_{ijkl}\, \varepsilon_{ij}(u)\varepsilon_{kl}(v) d\Omega
$$

$$
l(v,\phi) = \int_\Omega f.v d\Omega + \int_{\Gamma_N} g.v d\Gamma
$$

$$
\text{for all} \quad v \in U \quad, \quad u|_{\Gamma_D} = u_0
$$

where Ω is the structural domain and its boundary is represented by $\Gamma = \partial\Omega$. Also, the displacement field u_0 is the prescribed displacement on Γ_D; E_{ijkl} is the elasticity tensor; ε_{ij} the strain tensor; and f and g are body the force and surface load, respectively.

In the objective function $J(u)$, the first term is the mean compliance where the function $F(u) = 1/2 E_{ijkl}\varepsilon_{ij}(u)\varepsilon_{kl}(u)$ is the strain energy density, and ρ is the material density ratio. The second term of the objective function is the regularization β term and is a nonnegative value to control the effect of this term [16]. Furthermore, this term controls both the length of interfaces and the jump of ϕ may not be continuous in the piecewise constant level set method. H_1 defines the material fraction for different phases, and V_0 is the maximum admissible volume of the design domain. H_2 is the piecewise constant constraint to guarantee the level set function belong to only one phase [16].

Using the augmented Lagrangian method, the problem (9) can be converted into an unconstraint one as [16]:

$$
L(\phi,\lambda) = J(\phi) - a(u,v,\phi) + l(\phi,\lambda) + \lambda_1 H_1 + \frac{1}{2\mu_1} H_1^2 + \lambda_2 \int_\Omega H_2 d\Omega + \frac{1}{2\mu_2} \int_\Omega H_2^2 d\Omega \tag{10}
$$

where $\lambda_1 \in R$ and $\lambda_2 \in L^2(\Omega)$ are the Lagrange multiplier, and $\mu_1, \mu_2 > 0$ are penalty parameters.

For finding the saddle point of this function when there is no body force, f and the boundary traction, g, the following equation was proposed by Wei and Wang [16] as:

$$
\int_\Omega \Psi\left(u,\phi,\tilde{\lambda}_1,\tilde{\lambda}_2\right) \delta\phi d\Omega = 0 \tag{11}
$$

$$
\Psi\left(u,\phi,\tilde{\lambda}_1,\tilde{\lambda}_2\right) = \frac{1}{2}\rho'(\phi) E_{i,j,k,l}\varepsilon_{i,j}(u)\varepsilon_{k,l}(u) + \beta\nabla.\left(\frac{\nabla\phi}{|\nabla\phi|}\right) + \tilde{\lambda}_1\rho'(\phi) + \tilde{\lambda}_2 K'(\phi) \tag{12}
$$

where

$$\rho'(\phi) = \frac{\partial \rho(\phi)}{\partial \phi} = c_2 - c_1 \tag{13}$$

$$K'(\phi) = \frac{\partial K(\phi)}{\partial \phi} = 2\phi - 3 \tag{14}$$

and

$$\tilde{\lambda}_1 = \lambda_1 + \frac{1}{\mu_1}\left(\int_\Omega \rho(\phi)d\Omega - V_0\right) \tag{15}$$

$$\tilde{\lambda}_2 = \lambda_2 + \frac{1}{\mu_2}K(\phi) \tag{16}$$

In order to satisfy Eq. (11), the steepest descent method is used by selecting $\delta\phi$ as the following form [16]:

$$\delta\phi = \frac{d\phi}{dt} = -\Psi\left(u, \phi, \tilde{\lambda}_1, \tilde{\lambda}_2\right) \tag{17}$$

Now, the optimization problem can be transformed into an ordinary differential equation problem with initial value ϕ_0. The simplest manner for updating the level set function ϕ is to use the explicit update scheme [16]:

$$\phi^{n+1} = \phi^n + \frac{d\phi}{dt}\Delta t \tag{18}$$

In this study, a semi–implicit method with the additive operator splitting (AOS) scheme is used. Therefore, H_2 can be eliminated in Eq. (10) and is not required for update μ_2 and λ_2 associated with this constraint.

The Lagrange multiplier λ_1 and the penalty parameter μ_1 related to volume constraint with are also updated as [16]:

$$\lambda_1^{k+1} = \lambda_1^k + \frac{1}{\mu_1^k}\left(\int_\Omega \rho(\phi)dx - V_0\right)$$
$$\mu_1^{k+1} = \alpha\,\mu_1^k \tag{19}$$

where $\alpha \in (0,1)$ is a constant parameter.

3. AOS AND MBO SCHEMES IN TOPOLOGY OPTIMIZATION

3.1 The AOS scheme

For a given function space V and an operator (linear or nonlinear) defined in V, solving the following time dependent equation is required [16]:

$$\frac{\partial \phi}{\partial t} + A(\phi) = f(t), \quad t \in [0, T] \quad ; \quad \phi(0) = \hat{\phi} \in V \tag{20}$$

where V is a function space. By assuming the operator A as the time dependent, A and the function f can be splitted in the following form [16]:

$$A = A_1 + A_2 + ... + A_m \quad ; \quad f = f_1 + f_2 + ... + f_m \tag{21}$$

The computations of the fractional steps are independent of each other and some splitting schemes can be used to approximate the solution of Eq. (20). In this study, additive splitting scheme (AOS) proposed by Lu *et al*. [29] and Weickert *et al*. [30] is used. Assume, τ is time step and $\phi^0 = \hat{\phi}$. Thus, at each time level $t_j = j\tau$, $\phi^{j+\frac{i}{2m}}$ can be calculated in parallel for $i = 1, 2, ..., m$:

$$\frac{\phi^{j+\frac{i}{2m}} - \phi^j}{m\tau} + A_i \phi^{j+\frac{i}{2m}} = f_i(t_j)$$

$$\phi^{j+1} = \frac{1}{m} \sum_{i=1}^{m} \phi^{j+\frac{i}{2m}} \tag{22}$$

3.2 The MBO scheme

The MBO scheme was first proposed for approximating the motion of an interface by its mean curvature [31]. Furthermore, the MBO scheme was used as a splitting scheme for the phase field model and extended to image segmentation problems. The MBO scheme for the case of two regions can be considered as an algorithm expressed in the framework [31]:
1. Choose initial value $\phi(0) = 1$ or 2 and the time step τ.

2. Solve $\tilde{\phi}(t)$ from

$$\tilde{\phi}_t = \Delta\tilde{\phi}$$

$$\tilde{\phi}(t_n) = \phi(t_n) \quad \text{in} \ \ \Omega$$

$$\frac{\partial \tilde{\phi}}{\partial n} = 0 \quad \text{on} \ \ \partial\Omega \tag{23}$$

where $t_n = n\tau (n = 0, 1, 2, ...)$ and $t \in [t_n, t_{n+1}]$.

3. Set

$$\phi(t_{n+1}) = \begin{cases} 1 & \text{if } \tilde{\phi}(t_{n+1}) < 1.5 \\ 2 & \text{if } \tilde{\phi}(t_{n+1}) \geq 1.5 \end{cases} \tag{24}$$

For connecting between the MBO scheme and the splitting algorithm, it is required to clarify it as a phase field method [21]. Let u be the solution of

$$u_t = \varepsilon \Delta u - \frac{1}{\varepsilon} W'(u) \tag{25}$$

In this study, it is assumed as $W(\xi) = (\xi - 1)(\xi - 2)$. If the time splitting scheme is used for solving Eq. (25), solving the following two equations is required:

$$\begin{aligned} (a) \ \phi_t &= \varepsilon \Delta \phi \\ (b) \ \phi_t &= -\frac{1}{\varepsilon} W'(\phi) \end{aligned} \tag{26}$$

The rescaled solution $\phi(x, t_n / \varepsilon)$ of Eq. (26.a) is the solution of (23). When $\varepsilon \to 0^+$, the rescaled solution $\phi(x, t_n / \varepsilon)$ of (24.b) has two stable and stationary solutions (i.e. $\phi = 1$, $\phi = 2$) and unstable one ($\phi = 1.5$). If the unstable solution is eliminated, Eq. (24) gets.

3.3 Hybrid of the PCLS method and the MBO and AOS schemes

In this section, the solution of Eq. (20) is expressed by the AOS scheme. In order to increase the convergence speed and the efficiency of PCLS method, this method is combined with MBO scheme. $A(\phi) = -\psi$ can be splitted into a sum of two following equations [22]:

$$B(\phi) = -\beta \nabla(\frac{\nabla \phi}{|\nabla \phi|}) + \frac{1}{2} \rho' E_{ijkl} \varepsilon_{ij}(u) \varepsilon_{kl}(u) - \tilde{\lambda}_1 \rho' \tag{27}$$

$$C(\phi) = -\tilde{\lambda}_2 K'(\phi) \tag{28}$$

For the PCLS method in two phase fields, the function for the MBO projection is defined by [22]:

$$P(\phi) = \begin{cases} 1 & \text{if } \phi \leq 1.5 \\ 2 & \text{if } \phi > 1.5 \end{cases} \tag{29}$$

Also, B is splitted into the following form:

$$B_i(\phi) = -\beta D_i\left(\frac{D_i\phi}{|\nabla\phi|}\right) + \frac{1}{2}\rho' E_{ijkl}\varepsilon_{ij}(u)\varepsilon_{kl}(u) - \tilde{\lambda}_1\rho' \ ; \ i=1,2 \tag{30}$$

where D_i denotes the partial derivative with respect to x_i. Also, the following equation is considered as:

$$A = B_1 + B_2 + C \tag{31}$$

For using the AOS scheme (Eq. (20)) for splitting when the piecewise constant constraint H_2 is replaced by the MBO projection in two dimensional problems, it is required to use the following algorithm [22]:

1. Obtain $\phi^{n+\frac{i}{4}}$ in parallel for $i=1,2$ from.

$$\frac{\phi^{n+\frac{i}{4}} - \phi^n}{2\tau} = -\beta D_i\left(\frac{D_i\phi^{n+\frac{i}{4}}}{\left|\nabla\phi^{n+\frac{i}{4}}\right|}\right) + \frac{1}{2}\rho' E_{ijkl}\varepsilon_{ij}(u)\varepsilon_{kl}(u) - \tilde{\lambda}_1\rho' \ ; \ i=1,2 \tag{32}$$

2. Compute ϕ^{n+1} by:

$$\phi^{n+1} = \frac{1}{3}\left(p(\phi^n) + \sum_{i=1}^{2}\phi^{n+\frac{i}{4}}\right) \tag{33}$$

4. ISOGEOMETRIC ANALYSIS APPROACH

Isogeometric analysis (IGA) approach has been developed as a powerful computational approach that offers the possibility of integrating FE analysis into conventional NURBS–based CAD tools [24]. The IGA approach has attracted many attentions in various engineering problems, which has been applied for the discretization of partial differential equations. The main advantage of IGA is to use the NURBS basis functions which accurately model the exact geometries of solution space for numerical simulations of physical phenomena.

4.1 B–Spline and NURBS basis function

In this section, the B–Spline and NURBS basis function is expressed. A NURBS surface is parametrically defined as [32]:

$$S(\xi,\eta) = \frac{\sum_{i=1}^{n}\sum_{j=1}^{m} N_{i,p}(\xi)N_{j,q}(\eta)\omega_{i,j}P_{i,j}}{\sum_{i=1}^{n}\sum_{j=1}^{m} N_{i,p}(\xi)N_{j,q}(\eta)\omega_{i,j}} \tag{34}$$

where $P_{i,j}$ are (n,m) control points, $\omega_{i,j}$ are the associated weights and $N_{i,p}(\xi)$ and $N_{j,q}(\eta)$ are the normalized B–splines basis functions of degree p and q respectively. The i th B–splinebasis function of degree p, shown by $N_{i,p}(\xi)$, is expressed as [32]:

$$N_{i,0}(\xi) = \begin{cases} 1 & \text{if} \quad \xi_i \leq \xi < \xi_{i+1} \\ 0 & \text{otherwise} \end{cases} \tag{35}$$

and

$$N_{i,p}(\xi) = \frac{\xi - \xi_i}{\xi_{i+p} - \xi_i} N_{i,p-1}(\xi) + \frac{\xi_{i+p+1} - \xi}{\xi_{i+p+1} - \xi_{i+1}} N_{i+1,p-1}(\xi) \tag{36}$$

where $\xi = \{\xi_0, \xi_1, \ldots \xi_r\}$ is the knot vector and, ξ_i are a non–decreasing sequence of real numbers, which are called knots.

The knot vector $\eta = \{\eta_0, \eta_1, \ldots, \eta_s\}$ is employed to define the $N_{j,q}(\eta)$ basic functions for other direction. The interval $[\xi_0, \xi_r] \times [\eta_0, \eta_s]$ forms a patch [24]. A knot vector, for instance in ξ direction, is called open if the first and last knots have a multiplicity of $p+1$. In this case, the number of knots is equal to $r = n + p$. Also, the interval $[\xi_i, \xi_{i+1})$ is called a knot span where at most $p+1$ of the basic functions $N_{i,p}(\xi)$ are non–zero which are $N_{i-p,p}(\xi), \ldots, N_{i,p}(\xi)$.

4.2 formulation of isogeometric analysis based on NURBS

By using the NURBS basis functions for a patch p, the approximated displacement functions $u^p = [u, v]$ can be defined as [24]:

$$u^p(\xi, \eta) = \sum_{i=1}^n \sum_{j=1}^m R_{i,j}(\xi, \eta) u_{i,j}^p \tag{37}$$

where $R_{i,j}(\xi, \eta)$ is the rational term. Furthermore, the geometry is approximated by B–spline basis functions as [24]:

$$S^p(\xi, \eta) = \sum_{i=1}^n \sum_{j=1}^m R_{i,j}(\xi, \eta) S_{i,j}^p \tag{38}$$

By using the local support property of NURBS basis functions, Equations (37) and (38) can be summarized as it follows in any given $(\xi, \eta) \in [\xi_i, \xi_{i+1}) \times [\eta_j, \eta_{j+1})$.

$$u^p(\xi, \eta) = \left(u^p(\xi, \eta), v^p(\xi, \eta) \right) = \sum_{k=i-p}^i \sum_{l=j-q}^j R_{k,l}(\xi, \eta) U_{k,l}^p = \boldsymbol{RU} \tag{39}$$

$$S^p(\xi,\eta)=\left(x^p(\xi,\eta),y^p(\xi,\eta)\right)=\sum_{k=i-p}^{i}\sum_{l=j-q}^{j}R_{k,l}(\xi,\eta)P_{k,l}^p=\boldsymbol{RP} \qquad (40)$$

Final, the stiffness matrix for a single patch is also computed as,

$$\mathbf{K}=\iint_{\Omega}\mathbf{B}^T(\xi,\eta)\mathbf{D}\mathbf{B}(\xi,\eta)\left|\mathbf{J}\right|\bar{t}\,d\xi\,d\eta \qquad (41)$$

where $\bar{t}$ is the thickness, $\mathbf{B}(\xi,\eta)$ is the strain–displacement matrix, and $\mathbf{J}$ is the Jacobian matrix which maps the parametric space to the physical space. $\mathbf{D}$ is the elastic material property matrix for plane stress. It is noted that in this study the standard Gauss–quadrature over each knot space is utilized for numerical integration.

5. NUMERICAL EXAMPLES

To demonstrate the hybrid of the PCLS method and IGA approach for the 2–D topology optimization of structures, three examples of isotropic plane elasticity problem which have been widely studied in the relevant literature [22, 23, 25–27] are presented in this section. In all examples, the modulus of elasticity, the Poisson's ratio and thickness are considered as 1 *Pa*, 0.3 and1 *m*, respectively. In "Ersatz material" approach [15], Young's modulus of Ersatz material is assumed as $10^{-3}Pa$. Also, c_1 and c_2 are considered to be 0.001 and 1, respectively. In the optimization procedure, the size of time step was equal to be $\tau=9$, and the other parameters were considered as $\beta=10^{-6}, \lambda_1=0.01, \mu_1=500$ and $\alpha=0.9$. The initial level set function was considered to be constant with $\phi=2$.

5.1 Cantilever beam

The cantilever beam shown in Fig. 1 is selected as the first example. As shown in Fig. 1, the length of the domain is $L=80mm$ and the height is $H=40mm$. The cantilever is subjected to a concentrated load P=1N at the middle point of the free end.
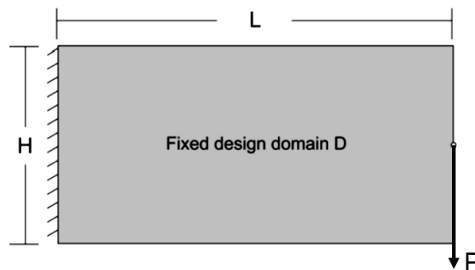

Figure 1. Fixed design domain and boundary condition of a cantilever example

In the optimization procedure, the volume constraint was assumed to be 40% of the total domain volume. Furthermore, the initial geometry was modeled based on a bi–quadratic NURBS geometry with 10×6 control points. The open knot vectors were respectively {0, 0, 0, 0.125, 0.25, 0.375, 0.5, 0.625, 0.75, 0.875, 1, 1, 1} and {0, 0, 0, 0.25, 0.5, 0.75, 1, 1, 1} in ξ and

η direction, thus leading to 8×4 knot spans. By subdividing each knot span into 10 equal parts in ξ and η direction, the physical mesh with 80×40 knot spans and the control mesh with 82×42 control points were obtained. The evolution procedure of the structural topology based on the proposed method is shown from Figs. 2(a) to 2(f). The final topology of the cantilever is also depicted in Fig. 2(f).
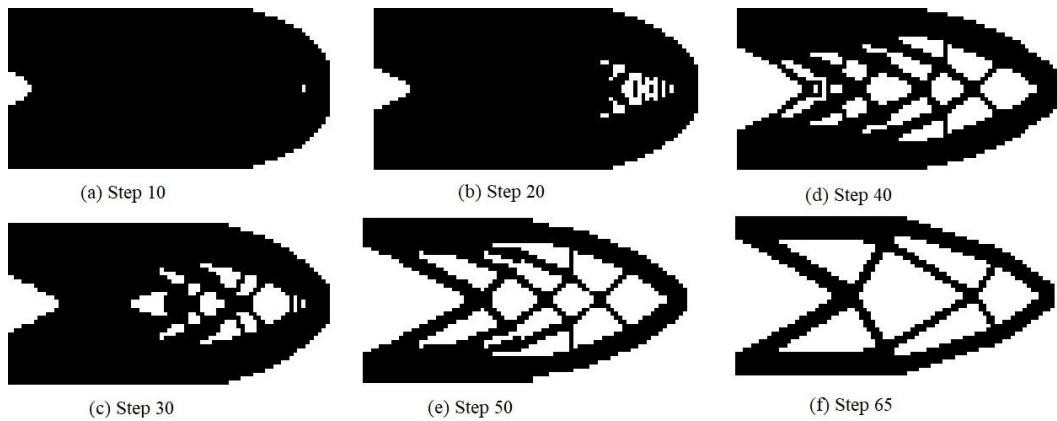

(a) Step 10   (b) Step 20   (d) Step 40

(c) Step 30   (e) Step 50   (f) Step 65

Figure 2. The evolution of optimal topology of the cantilever beam

In recent years, this example has been investigated by the other researchers [33–35]. The final optimal topology obtained the proposed method of this study was compared with those obtained in other studies [33–35] and shown in Fig. 3.
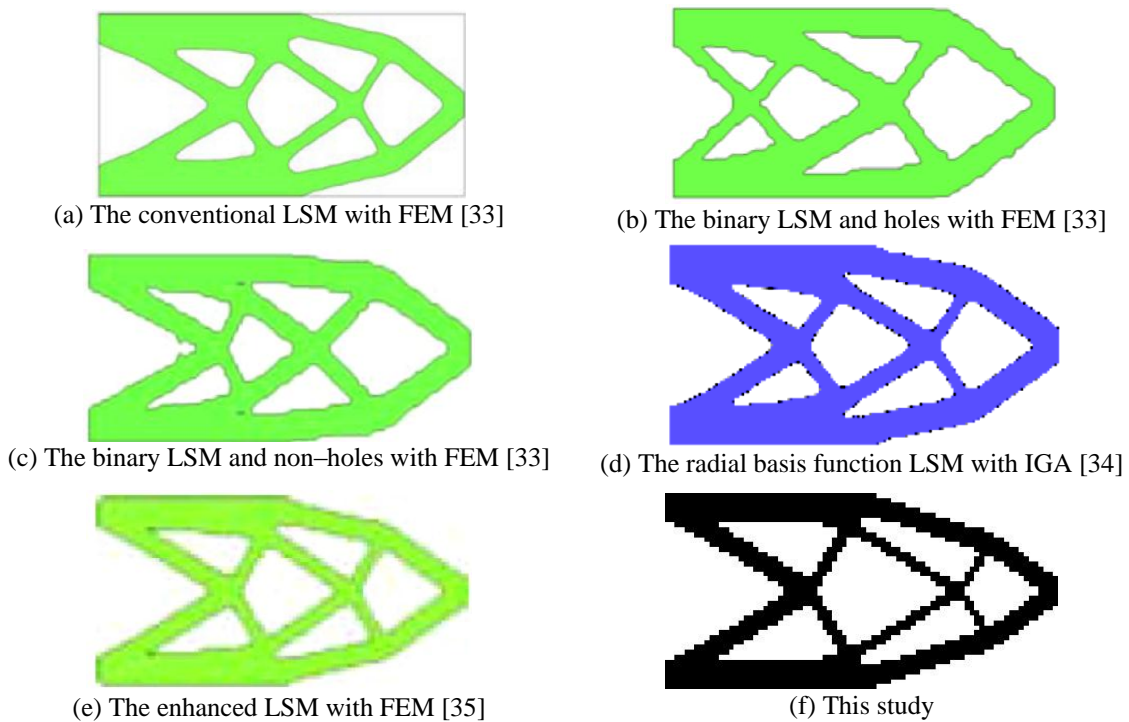

(a) The conventional LSM with FEM [33]   (b) The binary LSM and holes with FEM [33]

(c) The binary LSM and non–holes with FEM [33]   (d) The radial basis function LSM with IGA [34]

(e) The enhanced LSM with FEM [35]   (f) This study

Figure 3. The comparison of the final optimal topology in this study with the other studies

As can been seen from Fig. 3, the final design obtained in this study is similar to those reported in the literature. Furthermore, the optimal results of this study and other studies are compared and presented in Table 1.

Table 1: Comparison of the proposed method and other studies

Schemes	Objective function	Number of convergence iterations
The conventional LSM with FEM [33]	63.88	200
The binary LSM and holes with FEM [33]	62.73	115
The binary LSM and non–holes with FEM [33]	64.18	100
The radial basis function LSM with IGA [34]	62.66	60
The enhanced LSM with FEM [35]	80.22	81
The proposed method	74.70	65

It is obvious from Table 1 that the performance of the proposed method in the term of the number of convergence iterations is better than the other LSMs with FEM and IGA. Although, the radial basis function LSM with IGA [34] outperforms the proposed method. Hence, the proposed method can be considered as an efficient method in the structural topology optimization. The evolution of the compliance and the volume fraction are also shown in Fig. 4. The value of the compliance at the optimal design is equal to 74.70.
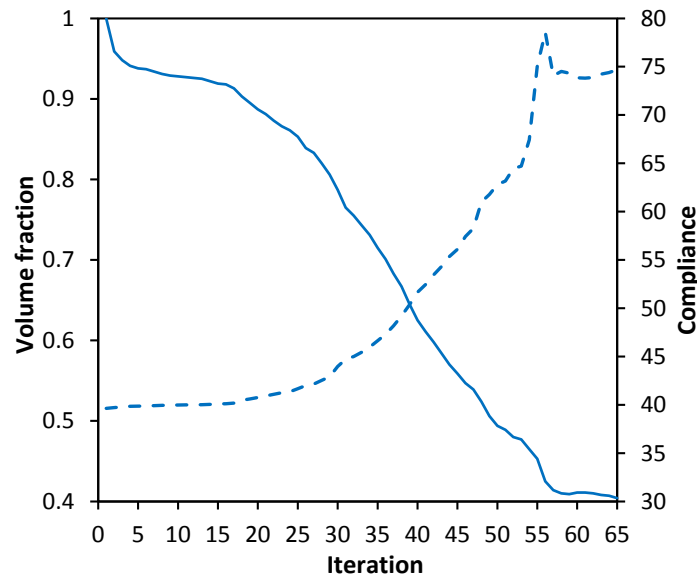

Figure 4. The convergence histories of the compliance and volume ratio

5.2 Messerschmitt–Bölkow–Blom beam

Messerschmitt–Bölkow–Blom (MBB) beam considered as the second example is the benchmark problem in the topology optimization of structures. The geometry model and loading conditions of the MBB beam is shown in Fig. 5. The length of the domain is $L = 120mm$ and the height is $H = 30mm$. The problem is subjected to a concentrated load

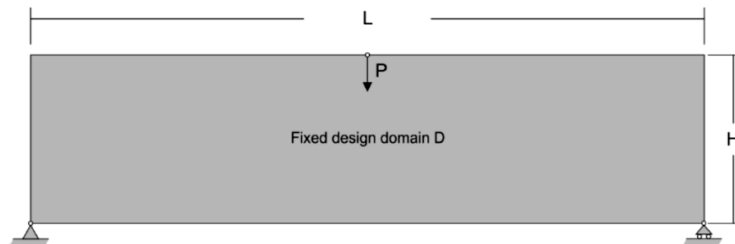P=1N at the upper half of the vane. In the optimization procedure, the specified material volume fraction is 40%.

Figure 5. Fixed design domain and boundary condition of the MBB beam

The topology optimization was implemented based on the proposed method with 120×30 mesh isogeometric and the topology evolving history was depicted in Fig. 6. The topology evolving history shown that the final topology was obtained in the 68 iterations.

(a) Step 10

(b) Step 20

(c) Step 30

(d) Step 40
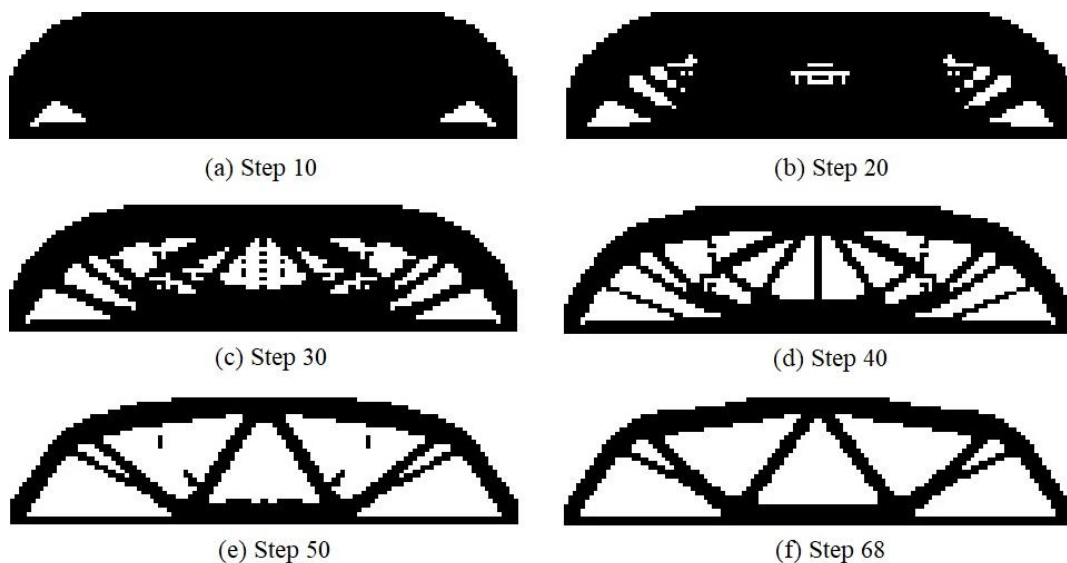
(e) Step 50

(f) Step 68

Figure 6. The evolution of optimal topology of the MBB beam

In order to validate the performance of the proposed method, the optimal topology obtained using the proposed method was also compared with that reported in the other studies and shown in Fig. 7. The comparison of the optimal topology shown in Fig. 7 reveals that the final topology obtained in this study is similar to those reported in the literature. Although, the trivial difference can be observed between the optimal topology obtained in this study and that reported in Ref. [35].

The optimal results of this study and the study implemented by Roodsarabi *et al*. [26] are compared in terms of the objective function and number of convergence iterations and reported in Table 2. As can be seen from Table 2, the performance of the proposed method in the term of the number of convergence iterations is better than the topological derivative–based LSM with FEM [26]. Although, the topological derivative–based LSM with IGA [26]

in comparison with the proposed method achieves a less compliance at a fewer number of convergence iterations. Hence, the proposed method can be considered as an efficient method in the topology optimization of the structure.
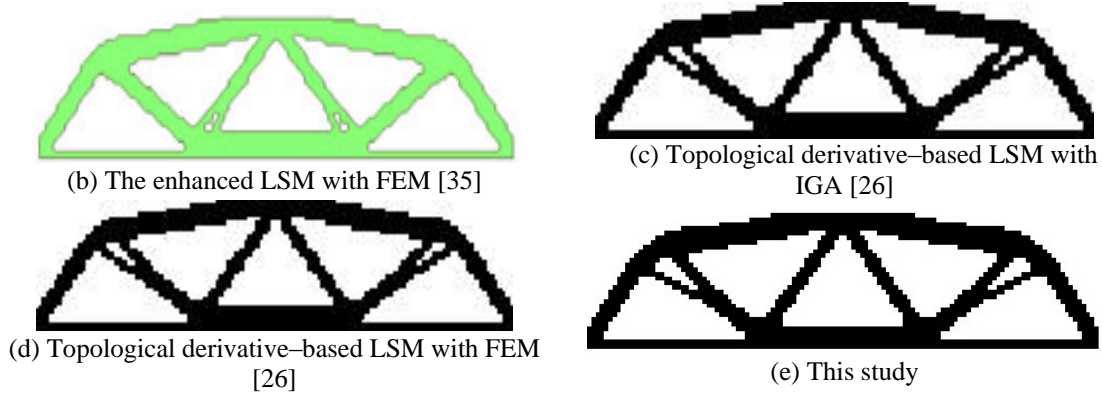

(b) The enhanced LSM with FEM [35]

(c) Topological derivative–based LSM with IGA [26]

(d) Topological derivative–based LSM with FEM [26]

(e) This study

Figure 7. The comparison of the final optimal topology in this study with the other studies

Table 2: Comparison of the proposed method and other LSMs

Schemes	Objective function	Number of convergence iterations
The topological derivative–based LSM with FEM [26]	46.94	70
The topological derivative–based LSM with IGA [26]	46.36	50
The proposed method	46.91	68

The history of the structural strain energy variation and material usage within the design domain during optimization is also depicted in Fig. 8.
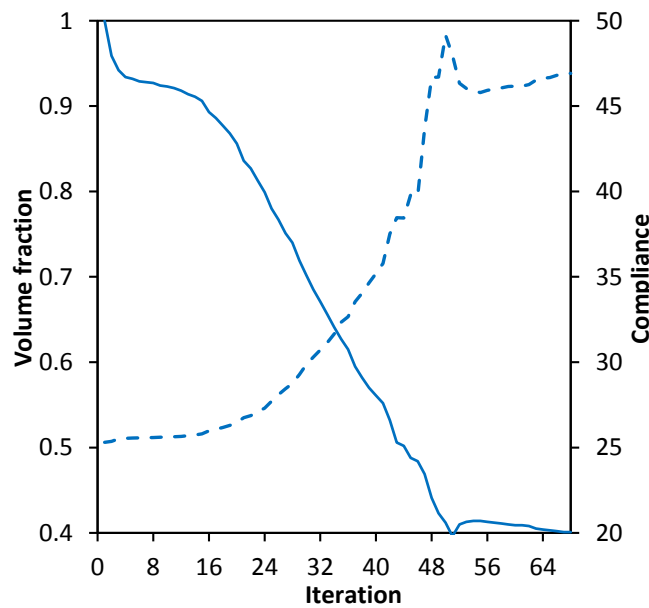

Figure 8. The convergence histories of the compliance and volume ratio

5.3 Michell structure with multiple loads

The Michell type structure with multiple loads was considered as the final example. Fig. 9 shows the boundary condition of this kind of structure. The left corner of the bottom of the design domain was fixed and its right corner was simply supported. Three forces were applied at the equal spaced point at the bottom boundary with $P_1 = 30N$ and $P_2 = 15N$. The design domain was 80×40 which is discretized with 3200, 1×1 squared elements. The volume fraction was assumed to be 40%.
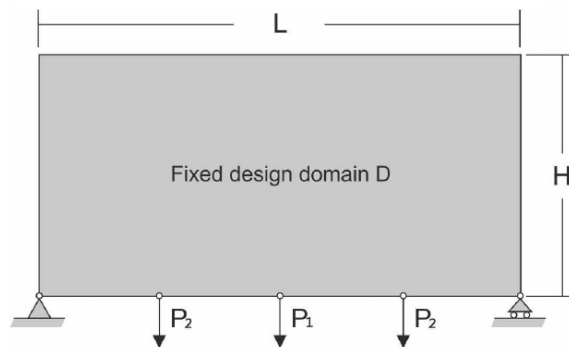

Figure 9. Fixed design domain and boundary condition of the Michell structure

The evolution process of the optimal topology of this Michell type structure is displayed in Fig. 10.

(a) Step 10

(b) Step 20

(c) Step 30
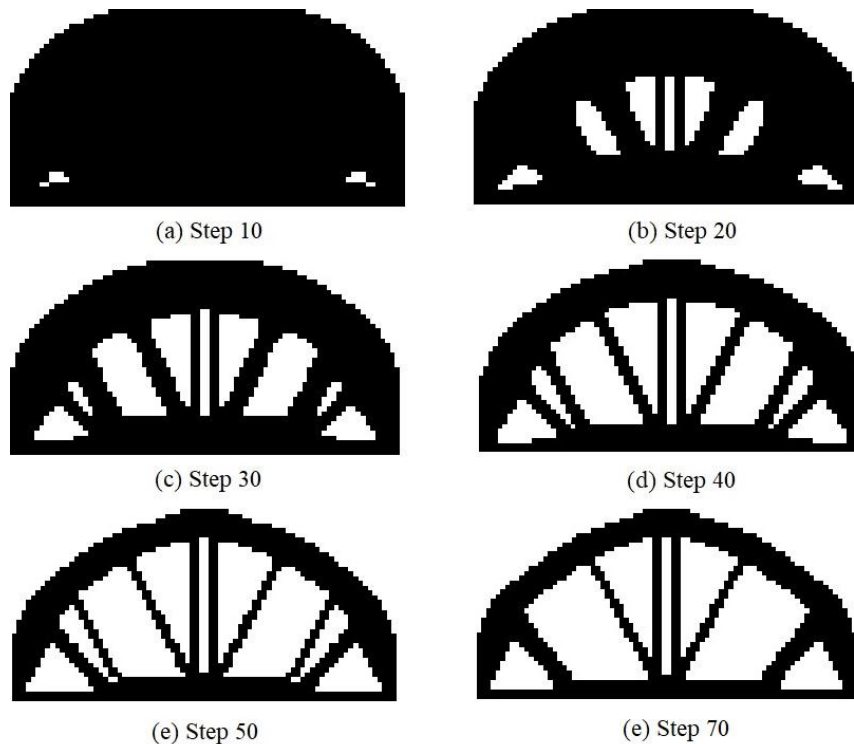
(d) Step 40

(e) Step 50

(e) Step 70

Figure 10. The evolution of the optimal topology for the Michell beam

The final topology was obtained in 70 iterations. For the assessment of the proposed method, the final optimal topology obtained in this study was compared with that obtained in the work of Shojaee and Moahmmadian [33] and was shown in Fig. 11. In the work of Shojaee and Moahmmadian [33], this example was investigated using the BLSM with FEM.

(a) The BLSM with FEM [33]   (b) This study
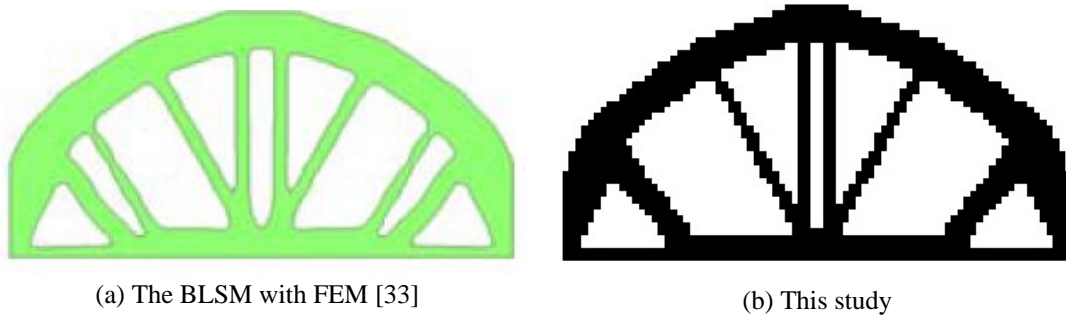
Figure 11. The comparison of the optimal topology in this study with that of Ref. [33]

As obvious from Fig. 11, the final design obtained in this study is approximately similar to that reported in the literature [33]. Furthermore, the comparison of the convergence history of the volume ratio and compliance between this study and the work of Shojaee and Moahmmadian [33] is shown in Figs. 12 and 13, respectively.

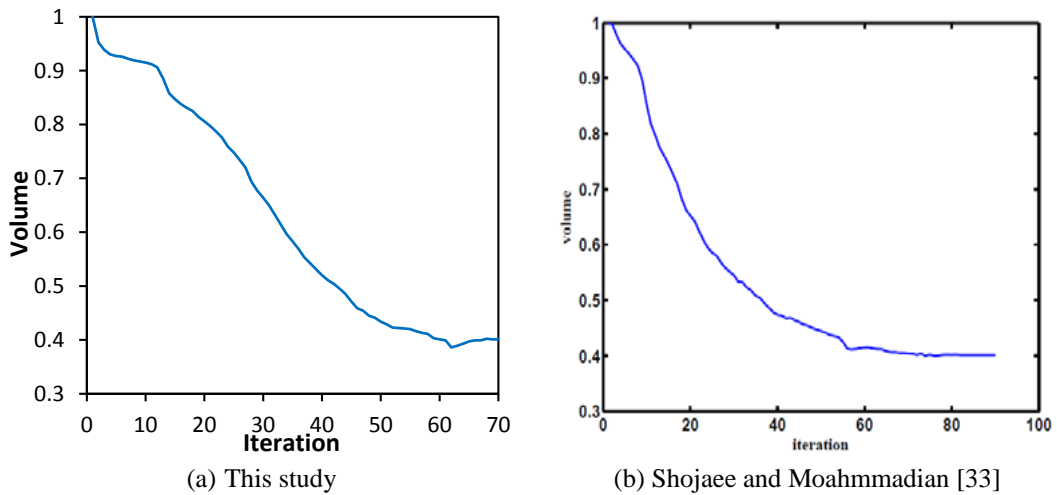(a) This study   (b) Shojaee and Moahmmadian [33]

Figure 12. The comparison of the convergence history of the volume ratio between this study and Ref. [33]

The results depicted in Figs. 12 and 13 demonstrated that the capability of the proposed method in the term of the number of convergence iterations is better than the BLSM with FEM.
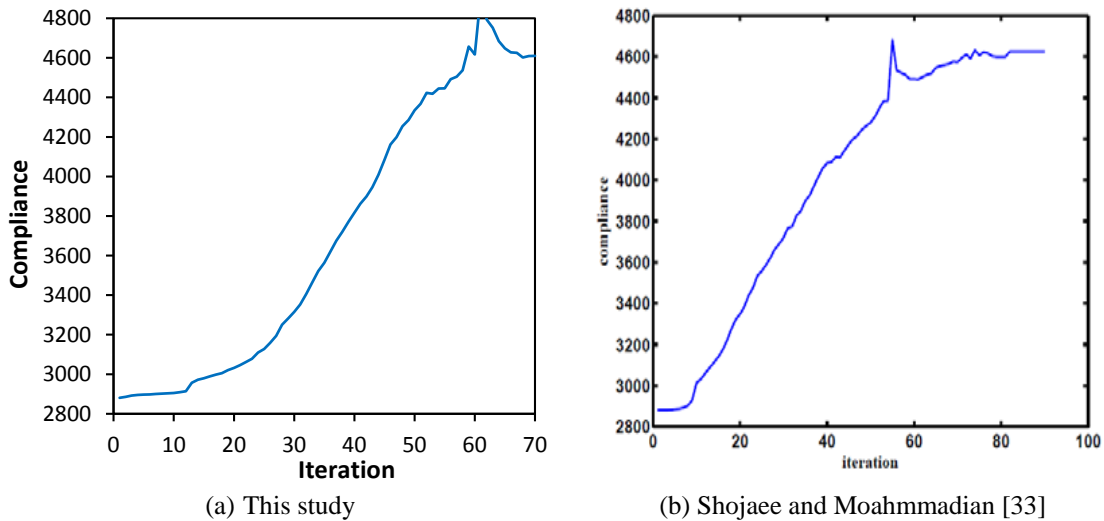
(a) This study   (b) Shojaee and Moahmmadian [33]

Figure 13. The comparison of the convergence history of the compliance between this study and Ref. [33]

6. CONCLUSIONS

The main aim of this study is to propose the hybrid of the PCLS method and the IGA approach for the topology optimization of structures. The PCLS method was related to both the classical LSMs and the phase–field methods. The piecewise constant constraint was used in the PCLS method for no overlap and vacuum between the sub–domains of different phases. In the conventional LSM, the augmented Lagrangian method as the penalization method has been considered, and it has required a tiny value for the penalty parameter. This causes that the convergence speed and numerical performance of the iterative procedure would become more challenging. In order to overcome these drawbacks, in this study the AOS scheme and the MBO projection were adopted in the PCLS method. In the topology optimization procedure, the NURBS based–IGA approach was also used instead of the conventional FEM.

The capability and efficiency of the proposed method was validated through the 2–D benchmark examples widely used in the structural topology optimization. For achieving this purpose, the number of convergence iterations and the final topology obtained by the proposed method was compared with the outcome of the other LSMs with FEM and IGA. The comparison of the proposed method and the other LSMs indicated that the PCLS method with IGA offered the similar optimal topology while requiring fewer convergence iterations. Although, the topological derivative–based LSM and the radial basis function LSM with IGA in comparison with the proposed method achieved a lighter volume ratio (or compliance) at a fewer number of iterations.

Further research is required to validate the robustness and efficacy of the proposed method in the 3–D structural topology optimization such as shell structures. Additional researches are also required to accurately determine its time complexity (or number of convergence iterations) in the 3–D structural topology optimization.

6. REFERENCES

1. Bendsoe MP, Kikuchi N. Generating optimal topologies in structural design using a homogenization method, *Comput Meth Appl Mech Eng* 1988; **71**: 97-224.
2. Rozvany GIN. *Structural Design via Optimality Criteria*, Kluwer Academic Publishers, Dordrecht, 1989.
3. Rozvany GIN, Zhou M. The COC algorithm, Part I: Cross section optimization or sizing, *Comput Meth Appl Mech Eng* 1991; **89**: 281–308.
4. Schmit LA, Farsi B. Some approximation concepts for structural synthesis, *AIAA J* 1974; **12**(5): 692–99.
5. Schmit LA, Miura H. *Approximation Concepts for Efficient Structural Synthesis*, NASA Publisher, Washington, United States, 1976.
6. Vanderplaats GN, Salajegheh E. A new approximation method for stress constraints in structural synthesis, *AIAA J* 1989; **27**(3): 352–58.
7. Svanberg K. The method of moving asymptotes–a new method for structural optimization, *Int J Numer Meth Eng* 1987; **24**: 359–73.
8. Tavakkoli SM, Hassani B, Ghasemnejad H. Isogeometric topology optimization of structures by using MMA, *Int J Optim Civil Eng* 2013; **3**: 313–26.
9. Kazemi HS, Tavakkoli SM, Naderi R. Isogeometric topology optimization of structures considering weight minimization and local stress constraints, *Int J Optim Civil Eng* 2016; **6**(2): 303–17.
10. Xie YM, Steven GP. A simple evolutionary procedure for structural optimization, *Comput Struct* 1993; **49**(5): 885–96.
11. Jakiela MJ, Chapman C, Duda J, Adewuya A, Saitou K. Continuum structural topology design with genetic algorithms, *Comput Meth Appl Mech Eng* 2000; **186**: 339–56.
12. Kaveh A, Hassani B, Shojaee S, Tavakkoli SM. Structural topology optimization using ant colony methodology, *Eng Struct* 2008; **30**(9): 2559–65.
13. Osher S, Sethian JA. Front propagating with curvature dependent speed: algorithms based on Hamilton–Jacobi formulations, *J Comput Phys* 1988; **78**: 12–49.
14. Sethian JA, Wiegmann A. Structural boundary design via level set and immersed interface methods, *J Comput Phys* 2000; **163**(2): 489–528.
15. Allaire G, Jouve F, Toader AM. Structural optimization using sensitivity analysis and a level set method, *J Comput Phys* 2004; **194**: 363–93.
16. Wei P, Wang MY. Piecewise constant level set method for structural topology optimization, *Int J Numer Meth Eng* 2009; **78**: 379–402.
17. Burger M, Hacker B, Ring W. Incorporating topological derivatives into level set methods, *J Comput Phys* 2004; **194**: 344– 362.
18. Wang SY, Wang MY. Radial basis functions and level set method for structural topology optimization, *Int J Numer Meth Eng* 2006; **65**: 60–90.
19. Wang SY, Wang MY. Structural shape and topology optimization using an implicit free boundary parameterization method, *Comput Model Eng Sci* 2006; **13**: 19–47.
20. Luo Z, Tong L, Luo J, Wei P, Wang MY. Design of piezoelectric actuators using a multiphase level set method of piecewise constants, *J Comput Phys* 2009; **228**: 2643–59.
21. Tai XC, Christiansen O, Lin P, SkjÆlaaen I. Image segmentation using some piecewise constant level set methods with MBO type of projection, *Int J Comput Vis* 2007; **73**: 61–76.

22. Shojaee S, Mohammadian M. Piecewise constant level set method for structural topology optimization with MBO type of projection, *Struct Multidisc Optim* 2011; **44**: 455–69.

23. Shojaee S, Mohaghegh A, Haeri A. Peiecwise constant level set method based finite element analysis for structural topology optimization using phase field method, *Int J Optim Civil Eng* 2015; **5**(4): 389–407.

24. Hughes TJR, Cottrell J, Bazilevs Y. Isogeometric analysis: CAD, finite elements, NURBS, exact geometry and mesh refinement. *Comput Meth Appl Mech Eng* 2005; **194**: 4135–95.

25. Roodsarabi M, Khatibinia M, Sarafrazi SR. Isogeometric topology optimization of structures using level set method incorporating sensitivity analysis, *Int J Optim Civil Eng* 2016; **6**(3): 405–22.

26. Roodsarabi M, Khatibinia M, Sarafrazi SR. Hybrid of topological derivative–based level set method and isogeometric analysis for structural topology optimization, *Steel Compos Struct* 2016; **21**(6): 1389–410.

27. Khatibinia M, Roodsarabi M, Barati M. topology optimization of plane structures using binary level set method and isogeometric analysis, *Int J Optim Civil Eng* 2018; **8**(2): 209–26.

28. Lie J, Lysaker M, Tai XC. *Piecewise Constant Level Set Methods and Image Segmentation. In Scale Space and PDE Methods in Computer Vision*, Lectures notes in Computer Sciences 3459, Springer, 2005, pp. 573–584.

29. Lu T, Neittaanmaki P, Tai, XC. A parallel splitting up method and its application to navier–stoke equations, *Appl Math Letter* 1991; **4**: 25–9.

30. Weickert J, Romeny BH, Viergever MA. Efficient and reliable schemes for nonlinear diffusion filtering, *IEEE Trans Image Process* 1998; **7**: 398–409.

31. Merriman B, Bence JK, Osher SJ. Motion of multiple functions: a level set approach, *J Comput Phys* 1994; **112**(2): 334–63.

32. Piegl L, Tiller W. *The NURBS Book*, Springer, 2nd edition, Germany, 1995.

33. Shojaee S, Mohamadian M, A binary level set method for structural topology optimization, *Int J Optim Civil Eng* 2011; **1**(1): 73–90.

34. Shojaee S, Mohamadian M, Valizadeh N. Composition of isogeometric analysis with level set method for structural topology optimization, *Int J Optim Civil Eng* 2012; **2**(1): 47–70.

35. Mohammadian M, Shojaee S, Binary level set method for structural topology optimization with MBO type of projection. *Int J Numer Meth Eng* 2012; **89**(5): 658–70.